BAMS Article

Sampled Together

Assessing the Value of Simultaneous Collocated Measurements for Optimal Satellite Configurations

C. E. Powell, Christopher S. Ruf, Scott Gleason, and Scot C. R. Rafkin

KEYWORDS:
Climate;
Instrumentation/sensors;
Remote sensing;
Satellite observations;
Climate services;
Planning

ABSTRACT: This work applies a quantitative metric in order to capture the relative representativeness of nonsimultaneous or noncollocated observations and quantify how these observations decorrelate in both space and time. This methodology allows for the effective determination of thresholding decisions for representative matchup conditions and is especially useful for informing future network designs and architectures. Future weather and climate satellite missions must consider a range of architectural trades to meet observing requirements. Frequently, fundamental decisions such as the number of observatories, the instruments manifested, and orbit parameters are determined based upon assumptions about the characteristic temporal and spatial scales of variability of the target observation. With the introduced methodology, representativity errors due to separations in space and time can be quantified without prior knowledge of instrument performance, and errors driven by constellation design can be estimated without model ingest or analysis.

SIGNIFICANCE STATEMENT: Dramatic changes in the space industry are enabling new architectures and business models for Earth observations. Historically, operational weather and climate satellites have been built on school bus–sized platforms, with multiple instruments comanifested on the same asset. With newer small-satellite technologies and miniaturized payloads, government agencies and private ventures alike are considering the utility of proliferated constellations. One of the many trades to consider is precisely how observations degrade in representativity when separated by space and time. We suggest an objective metric that can be applied to define optimal observing requirements and constellation design. This work also enables future architecture proposals to account for representativity error in their overall error budget and performance specifications.

https://doi.org/10.1175/BAMS-D-23-0198.1
Corresponding author: C. E. Powell, cepowell@umich.edu
In final form 3 November 2023

AFFILIATIONS: Powell—Department of Climate and Space Sciences and Engineering, University of Michigan, Ann Arbor, Michigan, and National Environmental Satellite Data and Information Service, National Oceanic and Atmospheric Administration, Silver Spring, Maryland; **Ruf**—Department of Climate and Space Sciences and Engineering, University of Michigan, Ann Arbor, Michigan; **Gleason**—Daaxa LLC, Boulder, Colorado; **Rafkin**—SouthWest Research Institute, Boulder, Colorado

It is often desirable to measure the Earth system from two or more different instruments at the same place and time. Simultaneous collocated measurements, otherwise known as matchups, frequently form the basis for calibration activities, science investigations, and operational retrievals. Satellite platforms offer a unique opportunity to capture collocated and simultaneous observations for extended periods of time. Many operational missions manifest multiple sensors onto the same satellite platform. Operational sea surface altimetry missions generally employ a radar altimeter as the primary mechanism to determine sea surface height, but due to uncertainties due to tropospheric delay, the radar is supplemented by a microwave radiometer to measure integrated atmospheric refractivity due to water vapor in the observing column to meet accuracy requirements (Donlon et al. 2021). Weather satellites utilize similar techniques to meet requirements. The NOAA–NASA Joint Polar Satellite System employs coaligned microwave and infrared sounders to retrieve atmospheric profiles. To ensure operational consistency, the scanning mechanisms between the infrared and microwave instruments are synchronized such that they share the same field of regard across the scan (Kim et al. 2014).

The same logic also extends to formation flying, where instruments are not manifested on the same platform, but rather on multiple platforms in nearby, coordinated orbits. In the early 2000s, NASA populated its A-Train constellation satellites, named for its compact assemblage of several Earth science missions in the afternoon sun-synchronous polar orbit. When *CloudSat* and *CALIPSO* joined the A-Train in 2006, five separate satellites would fly in formation over the same ground track within roughly a 15-min window (Stephens et al. 2002; Schoeberl 2002). The quick succession of satellites and near-simultaneous observations were critical to several science goals of the constellation.

The decision to comanifest instruments on a single satellite platform usually involves various trade studies to evaluate the relative costs, risks, and performance benefits of the design. While sharing two or more instruments on the same satellite platform is often the most intuitive way to achieve simultaneity and collocation, it can increase the system complexity, as well as the volume, mass, and power budgets of the spacecraft. These budgets are known to drive overall mission cost and execution risk. At the other end of the spectrum, recent advances in miniaturized sensors, small satellite platforms, and low-cost launch services have enabled constellations of proliferated sensors. These new capabilities enable constellation designs previously considered untenable or uneconomical. There are inherent challenges and risks with proliferated constellations, including cross calibration, formation maneuvers, and operating complexity.

The transformations in the space industry, including the development of new business models for collecting observations from space, combined with growing demand for enhanced weather and climate services, are fostering new conditions for government agencies to consider as they embark on the next generation of Earth observing architectures. NOAA is currently formulating

a new architecture for low-Earth orbit, the Near Earth Orbit Network (NEON), and is considering constellations that look very different from its legacy missions (Werner 2023). NEON Series One satellites will contain microwave and infrared sounders, while the manifest for Series Two is still undefined, and may contain instruments such as visible imagers or ozone profiles. The orbital planes and constellation size for NEON is still undetermined, but it is expected that the disaggregation of instruments will enable more observations at similar or reduced costs. This program marks a shift from the current generation of polar-orbiting weather satellites, the Joint Polar Satellite System, which hosts five instruments on a single truck-sized platform. NASA recently commissioned a study from the National Academies of Science, Engineering, and Medicine to assess the utility of hosting a number of Earth science payloads on a single large commercial platform (National Academies of Sciences, Engineering, and Medicine 2023).

One of the advantages of using multiple smaller satellite platforms for Earth observations is that on-orbit resources are limited, and often the constellation risk posture can be improved by disaggregating and distributing sensors across multiple platforms. This advantage can be traded off against the detrimental effects of representativity error.

A number of tools have been developed to facilitate constellation design, usually with defined objective functions, such as minimizing revisit time, maximizing coverage, or balancing cost and utility (Marcuccio et al. 2019; Williams et al. 2001; St. Germain et al. 2018; Nag et al. 2015). These considerations feature prominently in the development of Earth observing missions and frequently trade off with one another. However, often the most important questions for selecting an optimal architecture—the definition of threshold and objective revisit requirements for a given observation—are decided somewhat arbitrarily.

One of the primary metrics used to measure the utility of future observing systems, particularly for weather satellites, is a technique known as observing system simulation experiments (OSSEs) (Arnold and Dey 1986). OSSEs essentially use a high-resolution model of the atmosphere and Earth system as ground truth, which are then "measured" by realistic simulated observations that are assimilated into a known forecasting model (Hoffman and Atlas 2016). These experiments can provide significant insight into the forecast impact of certain types of future observations but can be labor intensive and computationally expensive to run (to illustrate, cf. Li et al. 2019, 2018; Christophersen et al. 2021). Some newer techniques, such as employing noncycling data assimilation for OSSEs, can minimize the computational burden (Privé et al. 2023). Other approaches that are less resource intensive, such as ensemble data assimilation (EDA) studies, measure a simulated observing system's impact on forecasts by characterizing the spread between ensemble members (Tan et al. 2007). Nevertheless, these studies are frequently individually tuned to the observing system being developed, and the utility is restricted to estimating improvements for forecasting users. Because of the number of variables inherent in these models, and the lack of standardization between techniques, it is difficult to make precise decisions about what utility is gained by changing the temporal or spatial coverage of future observation architectures. Further, these computational frameworks are not entirely applicable to nonforecasting applications of satellite observations, where a simple objective metric could guide requirements flow-down for observation representativity.

This work examines precisely how much representativity error is incurred when observations are separated in space and time, without a priori knowledge about the observing system or model at hand. As a result, it is a tool to empower observation planners with objective functions to make architecture trades. Further, when coupled with OSSEs, EDA studies, and other forecast skill metrics, it provides a more comprehensive assessment of a specific architecture selection.

Methodology

Formulation. The challenge of assimilating many different observations, which are often irregularly sampled in space and time, has been well documented since the advent of numerical

weather prediction over a century ago (Richardson 1922). Gandin introduced a number of innovations in objective analysis and optimum interpolation of fields, which moved away from purely mathematical polynomial fittings and incorporated statistical arguments for how parameters of interest might decorrelate in space and time (Gandin 1965). These optimal interpolations methods were further generalized for data assimilation purposes by Rutherford (1972), who incorporated short-term forecast error information to produce a blend of observations and model rather than the forecast alone as a first guess. Implicit in this work is the need to inform the process with autocorrelation functions that represent how observations at a particular place and time relate to model-predicted values on a numerical grid. Bretherton et al. (1976) extended the rapidly advancing optimal interpolation assimilation methods used for initializing weather models to guide the development of an oceanographic field experiment. It is this context in which we adopt the general approach of Bretherton et al.—not for an oceanographic experiment, but for satellite-based observations.

The basic premise is that given simple assumptions about the statistical behavior of any observable parameter, such as wind speed or sea surface temperature, one can measure the rate that this parameter decorrelates over space and time. The error from interpolation is then simply

$$\epsilon_x\left(\tau_{t,s}\right)=\sigma_x\sqrt{1-R_x\left(\tau_{t,s}\right)}, \tag{1}$$

where representativity error for parameter x is ϵ_x and is a function of either time lag τ_t or spatial lag τ_s, σ_x is the standard deviation of samples of x, and R_x is the autocorrelation of parameter x at lag $\tau_{t,s}$, where the subscript t represents the time lag, and the subscript s represents the spatial lag. This formulation makes general assumptions about the stationarity and isotropy of variance for the parameter of interest which are not necessarily true for the Earth system. There are many cases in which the statistical distribution and rate of decorrelation of weather and climate parameters are nonstationary, such as from seasonality or phase of teleconnections. Generally, the error in (1) can be calculated in any case where a representative decorrelation rolloff can be estimated. The correlation scale sizes and decorrelation behavior of various Earth parameters is extensively studied and readily accessible for many parameters. As a partial sampling, confer Colosi and Barnett (1990) (identifying characteristic spatial and temporal scales in surface pressure, sea surface temperature, and air temperature over the Southern Hemisphere via drifting buoys), White (1995) (measuring decorrelation scales of temperature at various depths in global oceans to design an in situ network to measure gyre-scale seasonal-to-interannual variability), Gille and Kelly (1996) (decorrelation scales of sea surface height of the Southern Ocean as measured from satellite altimeters), Kuragano and Kamachi (2000) (spatial and temporal scales of global ocean surface variability from the TOPEX/Poseidon mission), Chu et al. (2002) (decorrelation scales of temperature and salinity in the Japan Sea from in situ ocean profiles), Delcroix et al. (2005) (temporal and spatial decorrelation in sea surface salinity in tropics), Romanou et al. (2006) (decorrelation scales of latent and sensible heat fluxes in global oceans), Eden (2007) (eddy length scales of the North Atlantic derived from satellite altimetry), and McLean (2010) (correlation scales of global oceans derived from Argo floats).

This analysis treats temporal and spatial decorrelation separately, even though they are coupled in the Earth system. The rationale is twofold. First, this maintains the simplicity and generality of the representativity errors. Second, this assumption makes this metric much more useful for the task of designing satellite architectures. Architecture trades frequently feature orbit and constellation decisions that optimize various sampling characteristics in both space and time, which are also coupled by orbital dynamics. Instead of trying to determine the

dynamics of multiple coupled systems, this relaxation allows planners to set simple threshold and objective requirements in space and time for their trade studies.

Choice of data and study selection. The goal of this exercise is to demonstrate how we apply a known benchmark to determine satellite constellation architectures. In practice, care should be taken to ensure that the chosen benchmarks are, in fact, representative of the target phenomenology. In essence, (1) simply measures the error induced by the separation between samples in space and time in which natural variability may cause a different measurement to be obtained. The statistical meaning of (1) also suggests that any input data need to adequately resolve the target parameter both in scale and variability. The temporal and spatial resolutions should be considered as well as any processing performed that would otherwise impact the variability. There is no policy constraint on the source of data, provided that it is sufficiently representative of the dynamics at the appropriate scale and variability of a given phenomenon.

In certain cases, raw observation data may be advantageous over model or reanalysis data; in others, the reverse may be true. This claim warrants some explanation. We generally have a strong preference for using observation data when available and practical. But there are certain use cases in which model or reanalysis data may be more representative, easier to manipulate, or simply readily available where observations are not. For instance, remote sensing data are commonly resampled from the native instrument resolution to a standard grid in both space and time, which can have a significant impact on the representativity of the data (Schutgens et al. 2016; Schutgens et al. 2017). Further, the statistical behavior of raw observation data may be sensitive to quality control parameters, which may not be intuitive to unfamiliar users. Some phenomena, such as global submesoscale precipitation, is not well captured by any global observing system, and a high-resolution model may be more appropriate than any blended observation dataset. Finally, in certain cases, the convenience of a gridded reanalysis may prove decisive if it can be shown to adequately capture the variability and scales of the target phenomena.

For this exercise, we assume that we are designing an ocean observing system, with particular interest in surface parameters such as winds, sea surface temperature, air temperature, and surface air pressure. Our selection of data are purely illustrative for the demonstration of this technique, and we assert representativity in both scale and variability. For observation planners, care should be taken to ensure that the source of "ground truth" for target observables provide representative sampling at time scales and spatial resolution appropriate for the phenomena of interest and are otherwise well calibrated to ensure representative variability and dynamic range.

Temporal decorrelation. For temporal decorrelation analyses, we chose a moored marine buoy from NOAA's National Data Buoy Center (1971) due to its high temporal resolution, the quality and calibration of the sensors, and the continuity of observations from a single platform. For our analysis, we examined one year of observations from station 51004, located at 17°32′17″N, 152°13′48″W (approximately 205 nm or 380 km southeast of Hilo, Hawaii), which is a 3-m foam buoy with an updated SCOOP payload that reports meteorological parameters at 10-min intervals (Kohler et al. 2015).

As discussed above, the choice of environmental parameter and source data may have a significant impact on the representativeness of decorrelation scales. For instance, parameters such as precipitation are likely to have much shorter characteristic decorrelation scale sizes than sea surface temperature. It is assumed that the temporal decorrelation scales from station 51004 data are sufficiently representative to use as a benchmark for

determining satellite constellation objectives in this hypothetical. We opted to use buoy data instead of reanalysis or other model outputs because model time steps tend to be too coarse to capture the decorrelation behavior of our target parameters. Station 51004 was chosen due to its long duration of continuous data collection without equipment changes as well as its near-equatorial location, which highlights highly variable surface weather patterns. We acknowledge that the temporal decorrelation of these parameters may vary by location but assert that the hypothetical satellite architecture is driven by requirements for tropical latitudes. For observation planners, we suggest identifying "worst-case" decorrelation behavior to drive requirements (i.e., stations that capture phenomena that have large variability and decorrelate quickly), which will vary depending on the target of interest.

The autocorrelation for observations was calculated assuming wide-sense stationarity for lags of 10 min. The decorrelation behavior and the resulting representativity error is shown in Fig. 1.

Figure 1 is illustrative of several factors that observation planners should consider. Figure 1a shows the decorrelation behavior of several observed parameters as well as one derived parameter, the air–sea temperature difference, which is obtained by simple arithmetic subtraction of the near-surface air temperature from the sea surface temperature observations. Some environmental parameters, such as sea surface temperature, are slowly varying on the time scale of hours to days. Other parameters, such as surface air pressure, exhibit strong diurnal behavior. The air–sea temperature difference decorrelates at a much faster rate than either air temperature or sea surface temperature alone, suggesting that these parameters are decoupled on time scales of less than a day. Figure 1b shows how these decorrelation behaviors factor into absolute representativity error. For example, the representativity error of air temperature and of the air–sea temperature difference are

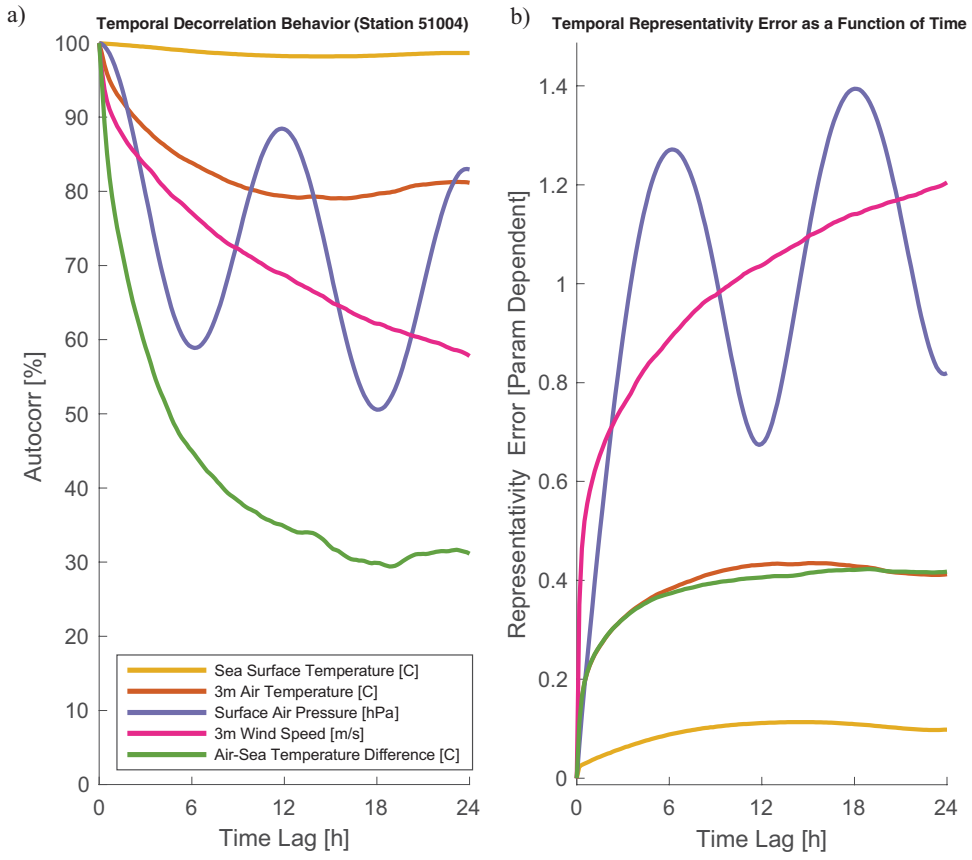

Fig. 1. (a) The temporal decorrelation behavior for a year of observations is demonstrated for various meteorological parameters from NDBC buoy station 51004. (b) The representativity error as calculated from (1) is shown. Note that the magnitude is dependent on the unit of measure.

nearly equivalent, despite the fact that the decorrelation behavior is vastly different. This is because the air–sea temperature difference has a much smaller dynamic range than the surface air temperature. At time lags of 5 h, both exhibit approximately 0.4°C of representativity error, but that value is much more significant for the air–sea temperature difference, which has a mean of −0.76°C and a standard deviation of 0.5°C.

It is important to emphasize that this formulation addresses only the component of matchup error due to representativity. The overall matchup error between two parameters should also include measurement and retrieval errors associated with the individual parameters. The representativity error can therefore be considered the floor for matchup accuracy of a given observing system.

Spatial decorrelation. A similar analysis can be applied in spatial dimensions. For a spatial dataset, we selected NASA's Modern-Era Retrospective Analysis for Research and Applications version 2 (MERRA-2) hourly, nonaveraged reanalysis (M2I1NXASM) (Gelaro et al. 2017; Global Modeling and Assimilation Office 2015). As before, we assume for this exercise that reanalysis data are sufficient to capture the spatial variability of our target parameters based on analysis from Gille (2005), which suggest that at tropical latitudes, the variability of ocean surface wind stress from reanalysis is consistent with observations from scatterometers. Ocean surface wind speed has the fastest decorrelation rolloff in our hypothetical study, but as before, this assumption should be reconsidered for other phenomena that vary at scale sizes smaller than the resolvability of the model.

Spatial decorrelation of ocean surface observations is known to be anisotropic and location dependent. This study adopts a simple solution frequently employed by oceanographers, which is to individually evaluate the meridional and zonal components of the spatial decorrelation scales of an ocean observation (White 1995; Reynolds and Smith 1994). For consistency, we center the meridional and zonal transects at the location of station 51004 as illustrated in Fig. 2. While these statistics are not stationary across the ocean, we assume for the purposes of this hypothetical that the statistics from station 51004 are representative.

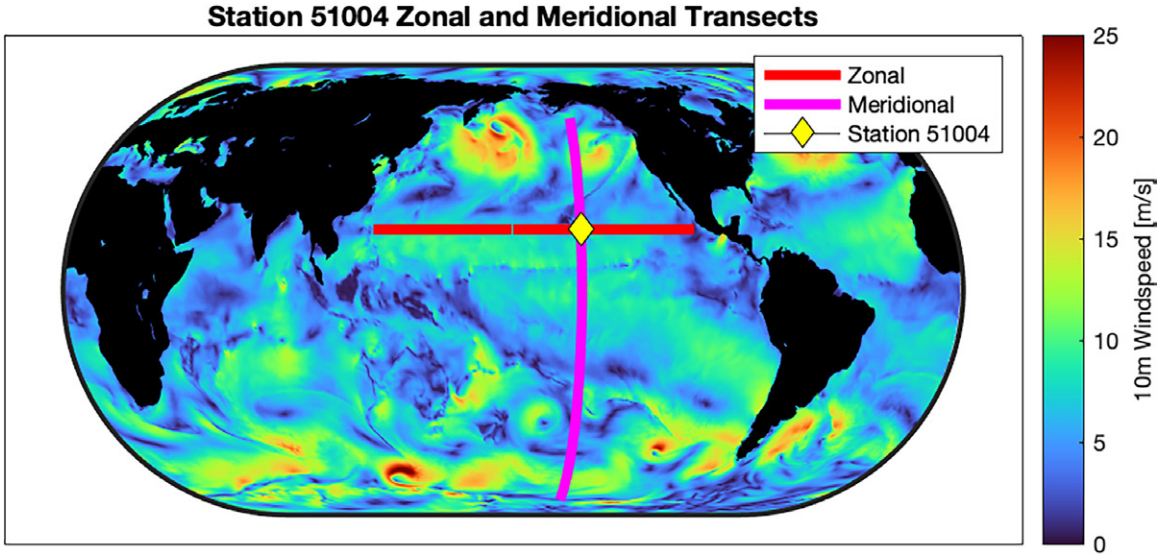

Fig. 2. The zonal and meridional transects for the Pacific basin centered at station 51004 are highlighted. The zonal transect consists of 210 grid cells at 0.625° spacing. The meridional transect consists of 254 grid cells at 0.5° spacing. The background field is of an initialization of MERRA-2's global wind speed output to emphasize that the spatial patterns of these parameters are quite different meridionally than they are zonally.

Figure 2 identifies which model grid cells are used to compute the zonal and meridional autocorrelation statistics. Because there are only 210 data points in the zonal transect and 254 data points in the meridional transect, the autocorrelation behavior derived from a single model run is somewhat noisy. To create a more representative decorrelation behavior, the autocorrelation is averaged across multiple model realizations over three months of data (at each hourly output for 92 days, or for 2,208 realizations).

Compared to the NDBC buoy data, the MERRA-2 hourly dataset produces slightly different observation parameters. For instance, the air temperature is the 10-m temperature, whereas the buoy data are observed at 3 m. Additionally we use the MERRA-2 skin temperature, which over most of the oceans is very similar to the sea surface temperature.

The average decorrelation behavior for the meridional and zonal transects centered at station 51004, as well as the implied representativity error, are shown in Fig. 3. Figure 3 reveals much about the spatial decorrelation behavior of the selected parameters. First, the behavior is substantially different between zonal and meridional transects, reflecting the spatial anisotropy in the decorrelation behavior in these parameters. Second, for the selected parameters, the spatial decorrelation rates suggest characteristic spatial scale sizes in the hundreds or even thousands of kilometers. Third, even when the decorrelation is comparable in zonal and meridional directions (i.e., the normalized autocorrelation is roughly equivalent for a given distance), the variability of the parameter may have significantly different magnitudes, changing the corresponding representativity error. For satellite missions, designers

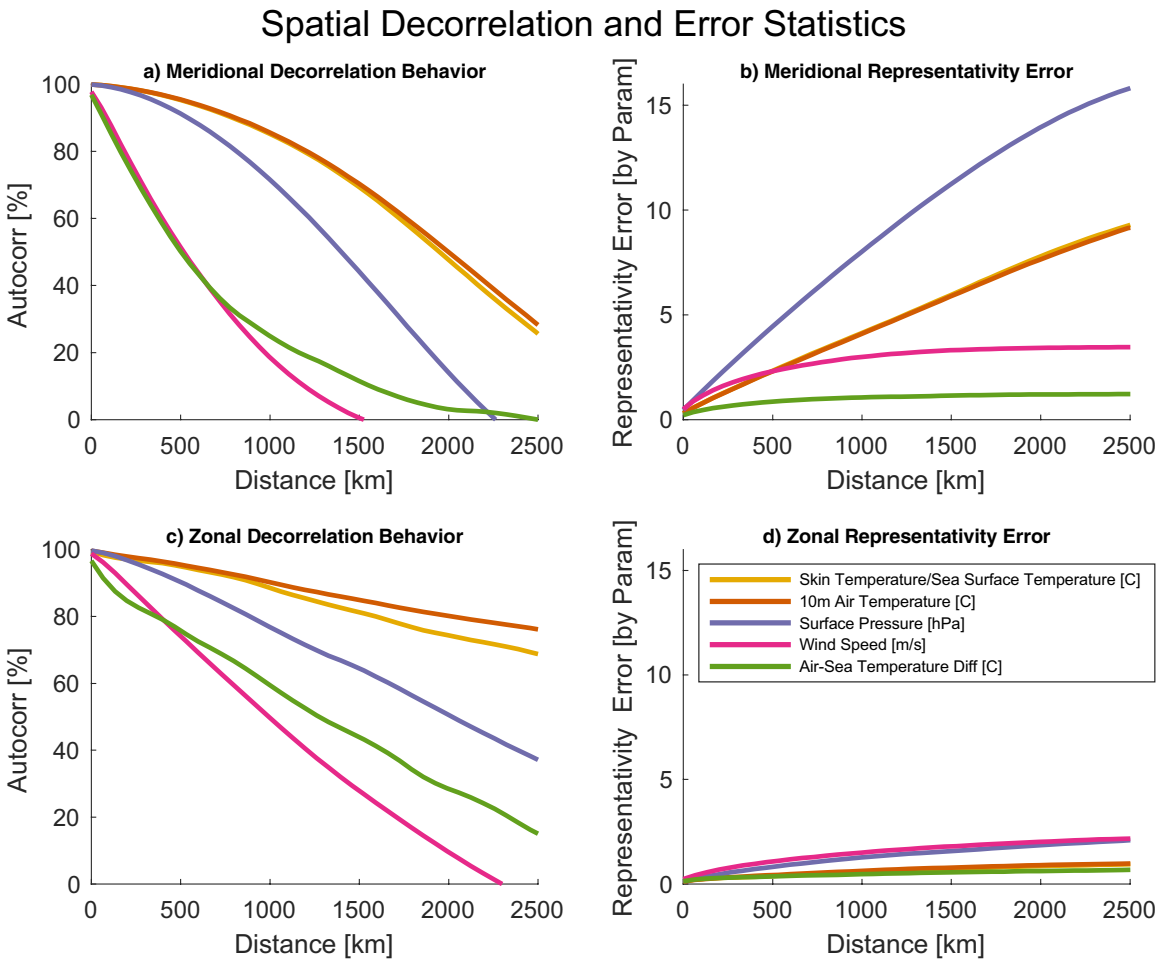

Fig. 3. The spatial decorrelation behavior and error statistics are partitioned into meridional and zonal components. (a) The meridional decorrelation behavior is shown for the specified environmental parameters. (b) The meridional representativity error is shown; note that the *y*-axis units are parameter dependent. (c) The zonal decorrelation behavior is shown for the specified environmental parameters. (d) The zonal representativity error is shown; note that the *y*-axis units are parameter dependent.

would want to base requirements decisions on the "worst-case" scenario, which may include regimes, conditions, and locations where the spatial representativity error grows the fastest. In the case of our hypothetical, that suggests that the meridional error statistics would generally drive architecture decisions.

Discussion

This technique enables observation planners to quickly estimate the representativity error caused by separations in observation space and time, which has widespread utility in planning future satellite constellations. Given appropriate and statistically representative datasets of planned observation targets, planners can set quantitative observation objectives for optimizing satellite constellations.

Shortcomings. It is worth repeating that the representativity error indicated in this analysis is not inclusive of the dominant error sources of most observing systems, such as ambiguity in the retrieval or noise from the sensor. In cases where the additional representativity error incurred by having nonsimultaneous and noncollocated measurements is small relative to the dominant error sources, it becomes reasonable to consider more flexible architectural approaches.

Further, there is danger in applying this technique with inappropriate input data that are not representative of the statistical behavior of the target parameter. Gridding observations can sometimes substantially impact the represented behavior. It can impose unwanted spectral filtering, changing the variability of the data, and can decrease the dynamic range of the data by smearing and averaging samples within gridded cells. Model and reanalysis data can be similarly nonrepresentative of the target phenomena, with a whole host of other computational and mechanical artifacts that can change the variability and scaling of model parameters.

As a statistical approach, this metric necessarily averages between "calm" low-variability periods and infrequent but high-variability events, which may be insufficient to capture the variability of dynamic and consequential phenomena, e.g., tropical cyclones. One could, however, restrict the distribution of input data to use only "worst-case" situations such as tropical cyclones as a design basis in order to estimate what spatial and temporal separation thresholds are needed to meet baseline representativity error requirements.

This technique also treats spatial and temporal dimensions separately, even though they are, in fact, coupled in the Earth system. This simplification is likely to impact conclusions drawn by a satellite observation planner in a conservative way. Decoupling spatial and temporal decorrelations will generally result in an overestimation of the error associated with spatial and temporal separations between samples. The decoupled results hence serve as a conservative upper bound on the error, and there may be opportunities to buy back more affordable satellite constellations with a coupled error estimate.

Utility and future work. We believe this metric should be considered by observation planners when considering architectural trade studies for new satellite constellations, and early in the mission life cycle when requirements are set. This simple metric can price when temporal resolution is too sparse for the assumption of simultaneity or when spatial coverage is too coarse for the assumption of collocation.

From our example, consider the design of a constellation to observe ocean surface wind speed from two separate observatories with the same orbit ground track. Given a requirement of representativity error no greater than 0.5 m s^{-1}, the above results from Fig. 1 indicate that the satellites be staggered no more than 25 min apart in the orbit plane. Note that this corresponds to an average representativity error under typical conditions. However, if the

target observable is ocean winds for tropical cyclone monitoring, during which surface wind speed exhibits a much larger dynamic range and steeper decorrelation rolloff, a 25-min separation would likely be too large. In this case, observation planners can quickly estimate that more satellites would be needed, and estimate cost of meeting this requirement. From another angle, planners with fixed budgets could mitigate this by placing the two satellites closer together within the same plane, reducing the revisit time between the two, but at the expense of daily coverage.

This problem can be extended to thresholds established for matching up observations for opportunistic or vicarious calibrations. Techniques such as simultaneous nadir overpasses (SNOs) (Zou et al. 2006) often establish thresholds in space and time that approximate simultaneity. This technique can establish objective representativity guidelines that can optimize the quantity of matchup data, or enable constellations that feature frequent SNOs for operational calibration.

Acknowledgments. We appreciate the thoughtful reviews for this manuscript, which substantially improved the readability and quality of this work. All remaining errors and deficiencies are the authors. This manuscript is the sole work of the listed authors and does not necessarily represent the views of the National Oceanic and Atmospheric Administration or the U.S. Department of Commerce. This work was partially supported by NASA Science Mission Directorate Contract NNL13AQ00C with the University of Michigan. The authors declare no conflict of interest.

Data availability statement. Data analyzed in this study were derived from existing public, openly available datasets cited in the reference section (see National Data Buoy Center 1971; Global Modeling and Assimilation Office 2015).

References

Arnold, C. P., and C. H. Dey, 1986: Observing-systems simulation experiments: Past, present, and future. *Bull. Amer. Meteor. Soc.*, **67**, 687–695, https://doi.org/10.1175/1520-0477(1986)067<0687:OSSEPP>2.0.CO;2.

Bretherton, F. P., R. E. Davis, and C. B. Fandry, 1976: A technique for objective analysis and design of oceanographic experiments applied to MODE-73. *Deep-Sea Res. Oceanogr. Abstr.*, **23**, 559–582, https://doi.org/10.1016/0011-7471(76)90001-2.

Christophersen, H. W., B. A. Dahl, J. P. Dunion, R. F. Rogers, F. D. Marks, R. Atlas, and W. J. Blackwell, 2021: Impact of TROPICS radiances on tropical cyclone prediction in an OSSE. *Mon. Wea. Rev.*, **149**, 2279–2298, https://doi.org/10.1175/MWR-D-20-0339.1.

Chu, P. C., W. Guihua, and Y. Chen, 2002: Japan sea thermohaline structure and circulation. Part III: Autocorrelation functions. *J. Phys. Oceanogr.*, **32**, 3596–3615, https://doi.org/10.1175/1520-0485(2002)032<3596:JSTSAC>2.0.CO;2.

Colosi, J., and T. P. Barnett, 1990: The characteristic spatial and temporal scales for SLP, SST, and air temperature in the Southern Hemisphere. *J. Appl. Meteor.*, **29**, 694–703, https://doi.org/10.1175/1520-0450(1990)029<0694:TCSATS>2.0.CO;2.

Delcroix, T., M. J. McPhaden, A. Dessier, and Y. Gouriou, 2005: Time and space scales for sea surface salinity in the tropical oceans. *Deep-Sea Res. I*, **52**, 787–813, https://doi.org/10.1016/j.dsr.2004.11.012.

Donlon, C. J., and Coauthors, 2021: The Copernicus Sentinel-6 mission: Enhanced continuity of satellite sea level measurements from space. *Remote Sens. Environ.*, **258**, 112395, https://doi.org/10.1016/j.rse.2021.112395.

Eden, C., 2007: Eddy length scales in the North Atlantic Ocean. *J. Geophys. Res.*, **112**, C06004, https://doi.org/10.1029/2006JC003901.

Gandin, L. S., 1965: *Ob'ektivnyi analiz meteorologicheskikh polei* (*Objective Analysis of Meteorological Fields*). Israel Program for Scientific Translations, 242 pp.

Gelaro, R., and Coauthors, 2017: The Modern-Era Retrospective Analysis for Research and Applications, version 2 (MERRA-2). *J. Climate*, **30**, 5419–5454, https://doi.org/10.1175/JCLI-D-16-0758.1.

Gille, S. T., 2005: Statistical characterization of zonal and meridional ocean wind stress. *J. Atmos. Oceanic Technol.*, **22**, 1353–1372, https://doi.org/10.1175/JTECH1789.1.

——, and K. A. Kelly, 1996: Scales of spatial and temporal variability in the Southern Ocean. *J. Geophys. Res.*, **101**, 8759–8773, https://doi.org/10.1029/96JC00203.

Global Modeling and Assimilation Office, 2015: MERRA-2 inst1_2d_asm_Nx: 2D, 3-hourly, instantaneous, single-level, assimilation, single-level diagnostics, version 5.12.4. NASA Goddard Earth Sciences Data and Information Services Center, accessed 17 May 2023, https://doi.org/10.5067/3Z173KIE2TPD.

Hoffman, R. N., and R. Atlas, 2016: Future observing system simulation experiments. *Bull. Amer. Meteor. Soc.*, **97**, 1601–1616, https://doi.org/10.1175/BAMS-D-15-00200.1.

Kim, E., C.-H. J. Lyu, K. Anderson, R. V. Leslie, and W. J. Blackwell, 2014: S-NPP ATMS instrument prelaunch and on-orbit performance evaluation. *J. Geophys. Res. Atmos.*, **119**, 5653–5670, https://doi.org/10.1002/2013JD020483.

Kohler, P. E. C., L. LeBlanc, and J. Elliott, 2015: SCOOP—NDBC's new ocean observing system. *OCEANS 2015*, Washington, DC, IEEE, https://doi.org/10.23919/OCEANS.2015.7401834.

Kuragano, T., and M. Kamachi, 2000: Global statistical space-time scales of oceanic variability estimated from the TOPEX/Poseidon altimeter data. *J. Geophys. Res.*, **105**, 955–974, https://doi.org/10.1029/1999JC900247.

Li, Z., and Coauthors, 2018: Value-added impact of geostationary hyperspectral infrared sounders on local severe storm forecasts—Via a quick regional OSSE. *Adv. Atmos. Sci.*, **35**, 1217–1230, https://doi.org/10.1007/s00376-018-8036-3.

——, and Coauthors, 2019: The alternative of CubeSat-based advanced infrared and microwave sounders for high impact weather forecasting. *Atmos. Ocean. Sci. Lett.*, **12**, 80–90, https://doi.org/10.1080/16742834.2019.1568816.

Marcuccio, S., S. Ullo, M. Carminati, and O. Kanoun, 2019: Smaller satellites, larger constellations: Trends and design issues for Earth observation systems. *IEEE Aerosp. Electron. Syst. Mag.*, **34**, 50–59, https://doi.org/10.1109/MAES.2019.2928612.

McLean, L. M., 2010: The determination of ocean correlation scales using Argo float data. Ph.D. thesis, University of Southampton, 210 pp.

Nag, S., J. LeMoigne, D. W. Miller, and O. De Weck, 2015: A framework for orbital performance evaluation in distributed space missions for Earth observation. *2015 IEEE Aerospace Conf.*, Big Sky, MT, IEEE, https://doi.org/10.1109/AERO.2015.7119227.

National Academies of Sciences, Engineering, and Medicine, 2023: *Assessment of Commercial Space Platforms for Earth Science Instruments.* National Academies Press, 66 pp., https://doi.org/10.17226/27019.

National Data Buoy Center, 1971: Meteorological and oceanographic data collected from the National Data Buoy Center Coastal-Marine Automated Network (C-MAN) and moored (weather) buoys. NOAA National Centers for Environmental Information, accessed 17 May 2023, www.ncei.noaa.gov/archive/accession/NDBC-CMANWx.

Privé, N. C., M. McLinden, B. Lin, I. Moradi, M. Sienkiewicz, G. M. Heymsfield, and W. McCarty 2023: Impacts of marine surface pressure observations from a spaceborne differential absorption radar investigated with an observing system simulation experiment. *J. Atmos. Oceanic Technol.*, **40**, 897–918, https://doi.org/10.1175/JTECH-D-22-0088.1.

Reynolds, R. W., and T. M. Smith, 1994: Improved global sea surface temperature analyses using optimum interpolation. *J. Climate*, **7**, 929–948, https://doi.org/10.1175/1520-0442(1994)007<0929:IGSSTA>2.0.CO;2.

Richardson, L. F., 1922: *Weather Prediction by Numerical Process.* 1st ed. Cambridge University Press, 236 pp.

Romanou, A., W. B. Rossow, and S.-H. Chou, 2006: Decorrelation scales of high-resolution turbulent fluxes at the ocean surface and a method to fill in gaps in satellite data products. *J. Climate*, **19**, 3378–3393, https://doi.org/10.1175/JCLI3773.1.

Rutherford, I. D., 1972: Data assimilation by statistical interpolation of forecast error fields. *J. Atmos. Sci.*, **29**, 809–815, https://doi.org/10.1175/1520-0469(1972)029<0809:DABSIO>2.0.CO;2.

Schoeberl, M. R., 2002: The afternoon constellation: A formation of Earth observing systems for the atmosphere and hydrosphere. *IEEE Int. Geoscience and Remote Sensing Symp.*, Toronto, ON, Canada, IEEE, 354–356, https://doi.org/10.1109/IGARSS.2002.1025038.

Schutgens, N. A. J., E. Gryspeerdt, N. Weigum, S. Tsyro, D. Goto, M. Schulz, and P. Stier, 2016: Will a perfect model agree with perfect observations? The impact of spatial sampling. *Atmos. Chem. Phys.*, **16**, 6335–6353, https://doi.org/10.5194/acp-16-6335-2016.

——, S. Tsyro, E. Gryspeerdt, D. Goto, N. Weigum, M. Schulz, and P. Stier, 2017: On the spatio-temporal representativeness of observations. *Atmos. Chem. Phys.*, **17**, 9761–9780, https://doi.org/10.5194/acp-17-9761-2017.

Stephens, G. L., and Coauthors, 2002: The *CloudSat* mission and the A-Train: A new dimension of space-based observations of clouds and precipitation. *Bull. Amer. Meteor. Soc.*, **83**, 1771–1790, https://doi.org/10.1175/BAMS-83-12-1771.

St. Germain, K., F. W. Gallagher, and W. Maier, 2018: Opportunities highlighted by the NSOSA study. *2018 IEEE Int. Geoscience and Remote Sensing Symp.*, Valencia, Spain, IEEE, 7387–7390, https://doi.org/10.1109/IGARSS.2018.8517710.

Tan, D. G. H., E. Andersson, M. Fisher, and L. Isaksen, 2007: Observing-system impact assessment using a data assimilation ensemble technique: Application

to the ADM–Aeolus wind profiling mission. *Quart. J. Roy. Meteor. Soc.*, **133**, 381–390, https://doi.org/10.1002/qj.43.

Werner, D., 2023: NOAA kicks off NEON weather satellite program. SpaceNews, accessed 9 May 2023, https://spacenews.com/noaa-kicks-off-neon-weather-satellite-program/.

White, W. B., 1995: Design of a global observing system for gyre-scale upper ocean temperature variability. *Prog. Oceanogr.*, **36**, 169–217, https://doi.org/10.1016/0079-6611(95)00017-8.

Williams, E. A., W. A. Crossley, and T. J. Lang, 2001: Average and maximum revisit time trade studies for satellite constellations using a multiobjective genetic algorithm. *J. Astronaut. Sci.*, **49**, 385–400, https://doi.org/10.1007/BF03546229.

Zou, C.-Z., M. D. Goldberg, Z. Cheng, N. C. Grody, J. T. Sullivan, C. Cao, and D. Tarpley, 2006: Recalibration of Microwave Sounding Unit for climate studies using simultaneous nadir overpasses. *J. Geophys. Res.*, **111**, D19114, https://doi.org/10.1029/2005JD006798.